Eur. Phys. J. D (2020) 74: 48
https://doi.org/10.1140/epjd/e2019-100512-x

THE EUROPEAN PHYSICAL JOURNAL D

Regular Article

Deep minima in the Coulomb-Born triply differential cross sections for ionization of helium by electron and positron impact*

Cody M. DeMars, Jesse B. Kent[a], and Sandra J. Ward[b]

Department of Physics, University of North Texas, Denton, Texas 76203, USA

Received: 17 October 2019 / Received in final form 12 December 2019
Published online 17 March 2020

Abstract. Previously, a deep minimum in the measurements of the triply differential cross section (TDCS) for electron-helium ionization at an incident energy of 64.6 eV was interpreted in terms of a vortex. We apply the Coulomb-Born (CB1) and modified CB1 approximations to this process at the same incident energy and obtain a deep minimum whose position is in reasonable accord with time-dependent close-coupling results and experimental data. We also obtain the deep minimum in the TDCS that was measured for an energy of 74.6 eV. For both incident energies, but at slightly different gun angles to those used experimentally, we obtain a very deep minimum in the TDCS that is related to a vortex in the velocity field associated with the CB1 transition matrix element. We determine for energies of 44.6 eV–79.6 eV the gun and polar angles for a deep minimum in the CB1 TDCS. We apply both approximations to positron-helium ionization. For an incident energy of 205.25 eV we find a deep minimum in the TDCS that is related to a vortex in the velocity field associated with the CB1 transition matrix element.

1 Introduction

Murray and Read [1–3] measured the triply differential cross section (TDCS) for electron-impact ionization of helium in the doubly symmetric geometry where the two outgoing electrons have the same energy and same polar angle ξ with respect to the z-axis which bisects the angle 2ξ between the two outgoing electrons [4]. They varied the gun angle ψ, which is the angle between the detection plane (defined by the momenta of the two outgoing electrons) and the incident beam direction. Murray and Read [1] observed a deep minimum at $\psi = 67.5°$ and $\xi \approx 70°$ for a number of incident energies E_i (54.6 eV, 64.6 eV and 74.6 eV) and also a less deep minimum for $E_i = 44.6$ eV for $\psi = 60°$ and 75°. The minimum is the deepest for $E_i = 64.6$ eV. They suggested that the deep minima are possibly due to the interference between the scattering amplitudes for the forward- and backward-scattering processes [1].

The deep minimum in the TDCS for $E_i = 64.6$ eV has been confirmed by a number of calculations, although the values of ψ and ξ where the minimum occurs differs amongst the various calculations.

Using the product of three Coulomb waves for the final state wave function with dynamical screening (DS3C) [5], Berakdar and Briggs [4,5] confirmed that the TDCS has a deep minimum for $E_i = 64.6$ eV and $\psi = 67.5°$. The deep minimum occurred in their calculations around $\xi \approx 64°$ [4]. At $\xi = 64.23°$, the real and imaginary parts of the transition matrix element are both zero. Berakdar and Briggs [4] stated that, at the zero in the TDCS and where the real and imaginary parts of the transition matrix element are both zero, the coherent sum of all three terms in the transition matrix element must be zero.

Rasch et al. [6] performed a distorted wave calculation and concluded that the deep minimum is due to strong interference between incident and final channel distorted waves.

Colgan et al. [7] applied the three-body distorted-wave (3DW) and the time-dependent close-coupling (TDCC) methods to investigate the deep minima in the experimental measurements of the TDCS for electron-impact ionization of helium for $\psi = 67.5°$ and for the incident energies $E_i = 54.6$ eV and 64.6 eV, and also the minimum for $\psi = 75°$ and $E_i = 44.6$ eV. They interpreted the deep minimum for $E_i = 64.6$ eV in terms of deep destructive interference between different partial waves. The TDCC results agree remarkably well with the experimental measurements in the vicinity of minima, including the positions of the minima. The 3DW results show a dip in the TDCS for 64.6 eV but a strong minima for 44.6 eV and 54.6 eV [7]. For $E_i = 64.6$ eV, the minimum is deepest in their TDCC calculation for $\psi = 61.5°$ [7].

* Contribution to the Topical Issue "Low-Energy Positron and Positronium Physics and Electron-Molecule Collisions and Swarms (POSMOL 2019)", edited by Michael Brunger, David Cassidy, Saša Dujko, Dragana Maric, Joan Marler, James Sullivan, and Juraj Fedor.

[a] Work performed while an undergraduate student at UNT.
[b] e-mail: Sandra.Quintanilla@unt.edu

The DS3C [4,5], the distorted wave [6] and the TDCC [7] calculatons describe the deep minimum in the TDCS in terms of interference. However, Macek et al. [8] provided an explanation for the deep minimum in the experimental measurements of the TDCS for electron-impact ionization of helium at $E_i = 64.6$ eV [1,2] in terms of a vortex [9,10] in the velocity field associated with the ionization amplitude. (The velocity field that is associated with the wave function in coordinate space represents the motion of the probability density fluid [11,12]). Macek et al. [8] employed the DS3C method [4,5] and determined the ionization amplitude as a function of $\mathbf{k}_+ = (\mathbf{k}_a + \mathbf{k}_b)/2$, where $\mathbf{k}_a$ and $\mathbf{k}_b$ are the momenta of the two outgoing electrons. For $\psi = 67.5°$ used in the experiment [1–3], Macek et al. [8] obtained the minimum in the TDCS at $\xi = 62.5°$, but this minimum did not correspond to a zero in the ionization amplitude. However, they obtained a first-order zero for $\psi = 59.3°$ and $\xi = 60°$ and showed, that corresponding to this zero, there is a vortex in the velocity field associated with the ionization amplitude. For electron-helium ionization, Feagin derived a threshold-like analytical expansion of the scattering amplitude by considering the angular momentum of the electron pair about the vortex [13].

A deep minimum in the TDCS has been obtained for electron-impact ionization of a K-shell model carbon at an incident energy $E_i = 1801.2$ eV by Ward and Macek [14] using the Coulomb-Born (CB1) approximation [15–18]. This approximation gives the correct asymptotic high-energy limit for ionization for a fixed scattering angle and allows for the transfer of angular momentum [14]. At the deep minimum in the TDCS, there is a zero in the CB1 transition matrix element $T^{\rm CB1}_{\mathbf{k},1s}$ (where $\mathbf{k}$ is the momentum of the ejected electron). Corresponding to this zero there is a vortex in the velocity field associated with $T^{\rm CB1}_{\mathbf{k},1s}$ [14], namely $\mathbf{v} = \nabla_{\mathbf{k}} {\rm Im}[\ln T^{\rm CB1}_{\mathbf{k},1s}]$. Ward and Macek [14] showed that the $m = \pm 1$ dipole components of $T^{\rm CB1}_{\mathbf{k},1s}$ are necessary to obtain a zero in $T^{\rm CB1}_{\mathbf{k},1s}$.

Navarrete et al. [19] and Navarrete and Barrachina [20] interpreted a deep minimum in the fully differential cross section for positron-hydrogen ionization in terms of a vortex in the generalized velocity field $\mathbf{u}$. This field $\mathbf{u}$ is associated with the transition matrix element $T(\mathbf{k}_+, \mathbf{k}_-)$ according to $\mathbf{u} = \nabla_{\mathbf{k}_+,\mathbf{k}_-} {\rm Im}[\ln T]$, where $\mathbf{k}_+$ and $\mathbf{k}_-$ are the momentum of the scattered positron and ejected electron, respectively [19,20]. Interestingly, Navarrete and Barrachina [20,21] noticed that the velocity field rotates in opposite directions around two zeros in the transition matrix element and presented a vortex ring for an incident positron energy of 275 eV [22].

Very recently, Alrowaily et al. [23] noted that the extended velocity field associated with the positronium (Ps)-formation scattering amplitude for positron-hydrogen collisions in the Ore gap also rotates in opposite directions around the two zeros that they obtained in the amplitude.

One can in principle measure experimentally a deep minimum in a TDCS that corresponds to a zero in the ionization transition matrix element and relate this minimum to a vortex in the velocity field associated with the element. Importantly, angular momentum is associated with vortices. The expectation value of angular momentum does not vanish when ones considers a small area that includes the zero in the ionization transition matrix element [11,14,23,24]. Thus, one can connect a zero in the transition matrix element (a complex function) to angular momentum [14,24]. A literature survey of deep minima (zeros) in differential cross sections that are attributed to vortices in velocity fields can be found in references [14] and [23]. References [9–12,14,23,24] discussed velocity fields and vortices in these fields. Reference [9] presented vortices that occur in pairs with opposite circulation. A hydrodynamical interpretation of angular momentum and energy transfer in atomic processes is given in reference [25].

A goal of our work is to see whether there is a zero in $T^{\rm CB1}_{\mathbf{k},1s}$ for positron-impact ionization of helium and thus in the CB1 and modified CB1 TDCSs. A first-order zero in $T^{\rm CB1}_{\mathbf{k},1s}$ means that there is a vortex in the velocity field associated with $T^{\rm CB1}_{\mathbf{k},1s}$ and a circulation of $\pm 2\pi$. We first apply the CB1 and modified CB1 approximations to compute the TDCS for electron-impact ionization of helium at 64.6 eV where there are both experimental measurements [1–3] and an accurate TDCC calculation [7].

In this paper, for both electron- and positron-impact ionization of helium, we compute $T^{\rm CB1}_{\mathbf{k},1s}$ and the CB1 and modified CB1 TDCSs [26–28]. We find that the deep minima in the TDCS for electron-impact ionization obtained experimentally are close to the kinematics that give zeros in $T^{\rm CB1}_{\mathbf{k},1s}$. By slightly varying the gun angle ψ, we obtain zeros in the $T^{\rm CB1}_{\mathbf{k},1s}$ that corresponds to very deep minima in the TDCSs and to vortices in the velocity field associated with $T^{\rm CB1}_{\mathbf{k},1s}$ [14]. Furthermore, we also obtain a deep minimum in the TDCS for positron-impact ionization of helium that we relate to a vortex in the velocity field associated with $T^{\rm CB1}_{\mathbf{k},1s}$.

Helium is accessible experimentally for ionization by positron impact as well as by electron impact. Indeed, the TDCS has been measured for positron-helium ionization to investigate electron capture to the continuum [29], but not for the geometry or energy where we obtain theoretically a deep minimum in the TDCS. Other than our calculations, we are not aware of calculations of the TDCS for electron-helium ionization for $E_i = 74.6$ eV and for the out-of-plane doubly symmetric geometry. We are also not aware of results, other than ours, for the TDCS for positron-impact ionization at 205.25 eV.

The CB1 calculation is very fast to run compared to more elaborate TDCC and 3DW calculations, which enables us to run reasonably rapid systematic searches for zeros in the transition matrix element. Also, one expects that the velocity field would take less time to compute if one uses the CB1 approximation rather than more elaborate approximations such as the 3DW. Botero and Macek [16] noted that even though the CB1 approximation is a simple distorted wave approximation, for electron impact of helium in the coplanar symmetric geometry, the TDCS results agrees with experiment at

least as well as sophisticated distorted wave calculations [30,31].

In Section 2, we present the CB1 and modified CB1 approximations (Sec. 2.1) and the velocity field associated with $T^{\rm CB1}_{\mathbf{k},1s}$ (Sec. 2.2). In Section 3.1, we present the results for electron-helium ionization for incident energies and gun angles considered experimentally, as well as finding gun angles that give zeros in $T^{\rm CB1}_{\mathbf{k},1s}$ for different energies. We give the results for positron-helium ionization in Section 3.2 and summarize our findings in Section 4.

We use atomic units throughout unless explicitly stated otherwise, and we quote the angles in degrees and the incident energies E_i in eV.

2 Theory

2.1 Coulomb-Born and modified Coulomb-Born approximations

The Coulomb-Born (CB1) approximation was developed by Botero and Macek [15–17] for electron collisions from neutral atoms. The CB1 transition matrix element is the first non-zero term in a perturbative expansion of the transition matrix element.

Botero and Macek applied the CB1 approximation to electron-impact ionization of helium for different energies and geometries [16–18], including the coplanar symmetric geometry [16,18]. They found that the CB1 approximation gave reasonable agreement with experiment for an incident energy as low as 50 eV [17]. Furthermore, they introduced an improved final state Coulomb-Born approximation (ICBA) that included the normalization factor $N^-_{\mathbf{k}_{e^-e^-}}$ of the Coulomb wave $\psi^-_{\mathbf{k}_{e^-e^-}}$ for the two outgoing electrons, where $\mathbf{k}_{e^-e^-}$ is the relative momentum between the outgoing electrons. The ICBA TDCS agrees well in shape with the experimental TDCS in the coplanar geometry for energies close to threshold [18]. The ICBA is the specific modified Coulomb-Born approximation given in reference [32] where the Coulomb-Born wave function is multiplied by $N^-_{\mathbf{k}_{e^-e^-}}$. In our paper, we refer to the CB1 TDCS that is multiplied by the modulus squared of the normalization factor of the Coulomb wave for two outgoing particles (two electrons, or a scattered positron and an ejected electron) as the modified CB1 TDCS [18,32,33].

The direct CB1 transition matrix element $T^{\rm CB1}_{\mathbf{k},1s}$ for electron-impact ionization from a model atom where the electron is initially in a $1s$ state, is given by [15,16]

$$T^{\rm CB1}_{\mathbf{k},1s} = \langle \psi^-_{\mathbf{K}_f}(\mathbf{r}) \psi^-_{\mathbf{k}}(\mathbf{r}') \left| \frac{1}{|\mathbf{r}-\mathbf{r}'|} \right| \varphi_i(\mathbf{r}') \psi^+_{\mathbf{K}_i}(\mathbf{r}) \rangle \,, \qquad (1)$$

in which $\mathbf{k}$, $\mathbf{K}_i$ and $\mathbf{K}_f$ are the momentum of the ejected electron, the momentum of the incident electron, and momentum of the scattered electron, respectively. In equation (1), $\mathbf{r}$ and $\mathbf{r}'$ are respectively the position vector of the incident (or scattered) electron and of the atomic (or ejected) electron relative to the target nucleus.

Following the treatment of references [15,34], the $1s$ electron in the initial state is approximated by a ground-state hydrogenic wave function $\varphi_i(\mathbf{r}') = (1/\sqrt{\pi}) Z_T^{3/2} e^{-Z_T r'}$ with the screened target charge $Z_T = 1.3443$ chosen so that it gives the ionization energy of the $1s$ electron in He I $1s^2\,{}^1S_0$ [35]. Also, following reference [15], we set the effective charge $Z_{\rm eff}$ in the Coulomb wave functions for the incident and scattered electron to be equal to Z_T.

For the doubly symmetric geometry [1–3] and for $Z_{\rm eff} = Z_T$, the direct and exchange CB1 transition matrix elements are equal. Thus, for this situation, the CB1 TDCS for electron-helium ionization can be expressed as:

$$\frac{d^5\sigma^{\rm CB1}}{d\Omega_f dE_{\mathbf{k}} d\Omega_{\mathbf{k}}} = (2\pi)^4 \frac{2K_f k}{K_i} |T^{\rm CB1}_{\mathbf{k},1s}|^2 \,, \qquad (2)$$

where $d\Omega_{\mathbf{k}}$ is the solid angle for the ejected electron, $d\Omega_f$ is the solid angle for the scattered electron, and $E_{\mathbf{k}}$ is the energy of the ejected electron [14,15]. The factor of two on the right-hand side of equation (2) is due to there being two $1s$ electrons in the ground-state of helium.

For positron-impact ionization, we take $\mathbf{K}_i$ and $\mathbf{K}_f$ to be the momentum of the incident positron and momentum of the scattered positron, respectively, and we use appropriate sign of the charges.

2.2 Velocity field associated with the transition matrix element

Bialynicki-Birula et al. [9] discussed vortices in the velocity fields associated with atomic wave functions, whereas Macek [10] discussed vortices in the velocity field associated with the ionization amplitude. The velocity field $\mathbf{v}$ associated with $T^{\rm CB1}_{\mathbf{k},1s}$ for electron or positron ionization can be expressed as [14]:

$$\mathbf{v} = \nabla_{\mathbf{k}} {\rm Im}[\ln T^{\rm CB1}_{\mathbf{k},1s}] \,. \qquad (3)$$

For a first-order zero in $T^{\rm CB1}_{\mathbf{k},1s}$, there is a corresponding vortex in the velocity field associated with this element, and the circulation Γ is given by

$$\Gamma = \int_c \mathbf{v}\cdot\mathbf{d}\ell = \pm\mathbf{2}\pi \,. \qquad (4)$$

In this integral, the closed contour c is taken in an anticlockwise direction enclosing exactly one first-order zero in $T^{\rm CB1}_{\mathbf{k},1s}$ [8–10,14].

Near a first-order zero (z_0, x_0) in a complex function $f(z,x)$, such as the ionization transition matrix element or wave function, the function can be written in the form

$$f(z,x) \approx a[(z-z_0) + b(x-x_0)] = a[z' + bx'] \qquad (5)$$

where one takes ${\rm Im}[b] \neq 0$. In the vicinity of the zero, the dominant term of the velocity field, $\mathbf{v}_d$, for the ejection of an electron is given by

$$\mathbf{v}_d = \frac{{\rm Im}[b](\hat{\mathbf{x}}z' - \hat{\mathbf{z}}x')}{(z')^2 + |b|^2(x')^2 + 2{\rm Re}[b]z'x'} \qquad (6)$$

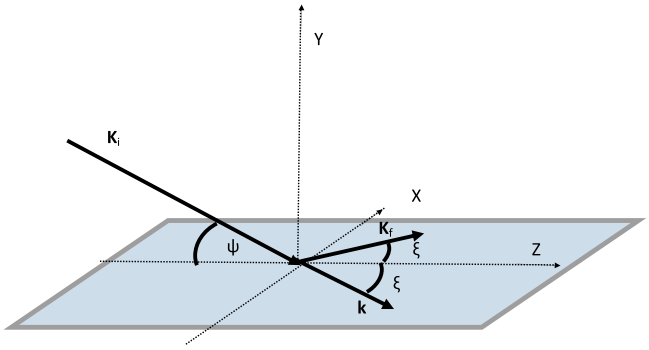

Fig. 1. Symmetric out-of-the plane geometry for electron-impact ionization of helium [1].

(see coordinates of Fig. 7) and the expectation value $\hat{y}$-component of the angular momentum operator for a small area A that includes the zero in $f(z,x)$ is given by [11,14,23,24]

$$\langle L_y \rangle_A = \frac{\int_A f^*(z,x) L_y f(z,x) dz'dx'}{\int_A |f(z,x)|^2 dz'dx'} \approx \frac{2\mathrm{Im}[b]}{1+|b|^2}. \quad (7)$$

Both of $\mathbf{v}_d$ and $\langle L_y \rangle_A$ are directly proportional to $\mathrm{Im}[b]$. For $\mathrm{Im}[b] > 0$ ($\mathrm{Im}[b] < 0$), the velocity field $\mathbf{v}$ circulates anticlockwise (clockwise) around the zero, $\Gamma = 2\pi$ (-2π) and $\langle L_y \rangle_A > 0$ (< 0).

3 Results

3.1 Deep minima in the TDCS for electron-impact ionization of helium

Following Murray and Read [1–3], we consider the doubly symmetric geometry (see Fig. 1) where the two outgoing electrons (whose momenta are $\mathbf{K}_f$ and $\mathbf{k}$ for the scattered and ejected electron, respectively) have the same energy and the same polar angle ξ [4]. The detection plane is the plane that is defined by the momenta of the two outgoing electrons, and the gun angle ψ is the angle between this plane and the momentum of the incident electron $\mathbf{K}_i$. The angle that the scattered electron makes with the z-axis is $\theta_f = \xi$, and the angle that the ejected electron makes is $\theta_k = -\xi$, so that the two electrons depart at angles of equal magnitude but opposite sign [16,18].

The experimental measurements [1–3] reveal a deep minimum in the TDCS of electron-impact ionization of helium at 64.6 eV. We compare in Figure 2 the CB1 and modified CB1 results with the measurements [1–3,36,37] and with the TDCC and 3DW results [7]. The TDCC method [7] can be used to test the reliability of the approximate methods in obtaining the deep minimum. The calculations from this method are in good agreement with the measurements in the shape of the TDCS and with the position of the deep minimum ($\xi \approx 70°$). The CB1 and modified CB1 results give a deep minimum but at $\xi = 76.3°$, which is at a larger angle than that obtained experimentally and from the TDCC calculations.

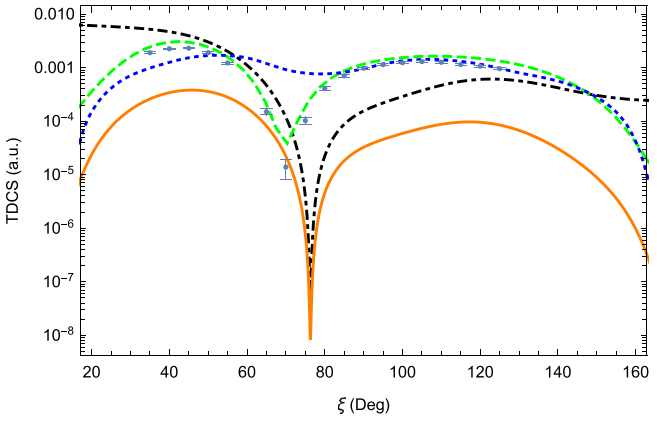

Fig. 2. The TDCS for electron-impact ionization of helium at 64.6 eV and a gun angle of 67.5°, verses the polar angle ξ, computed using the modified CB1 (the solid orange line), the CB1 (the black dot-dashed line), the 3DW (the blue dotted line) [7] and the TDCC (the green dashed line) [7] methods. The experimental results that have error bars are shown by blue data points [1–3,36,37].

We obtain the deepest minimum in the CB1 and modified CB1 TDCSs at $\psi = 67.88°$. This deep minimum is due to a zero in $T^{\mathrm{CB1}}_{\mathbf{k},1s}$ at $\xi = 76.3°$, and therefore a vortex in the velocity field $\mathbf{v}$ associated with $T^{\mathrm{CB1}}_{\mathbf{k},1s}$.

We determine the direct transition matrix element $T^{\mathrm{CB1}}_{\mathbf{k},1s}$ and the velocity field $\mathbf{v}$ associated with this element for a uniform grid in the z- and x-components (k_z, k_x) of $\mathbf{k}$ for $E_i = 64.6$ eV and for $\psi = 67.88°$. We consider the symmetric geometry of Figure 1 where both electrons have a polar angle of ξ. However, for the grid in (k_z, k_x), the energy of the scattered electron $E_f = K_f^2/2$ is adjusted appropriately so that the total energy of the system is conserved. In Figure 3 for this grid, we show a density plot of $\ln|T^{\mathrm{CB1}}_{\mathbf{k},1s}|$ and the nodal lines of $\mathrm{Re}[T^{\mathrm{CB1}}_{\mathbf{k},1s}]$ and $\mathrm{Im}[T^{\mathrm{CB1}}_{\mathbf{k},1s}]$. We also show by arrows the direction of the velocity field $\hat{\mathbf{v}}/|\mathbf{v}|$. We find that the velocity field, $\mathbf{v}$, rotates in an anticlockwise around the zero in $T^{\mathrm{CB1}}_{\mathbf{k},1s}$ which is at the intersection of the nodal lines and that the circulation is 2π. These results are consistent with $\mathrm{Im}[b] > 0$ which we obtain by fitting $T^{\mathrm{CB1}}_{\mathbf{k},1s}$ to the linear form of equation (5).

Murray and Read also obtained a deep minimum in their experimentally measured TDCS for electron-helium ionization for a higher incident energy of $E_i = 74.6$ eV but for the same gun angle of $\psi = 67.5°$ [1–3]. In Figure 4, we compare the CB1 and modified CB1 TDCSs with the experimental measurements [1–3,36,37]. As for the TDCS for electron-impact ionization of helium at a lower incident energy of 64.6 eV, the minimum in the CB1 and modified CB1 results ($\xi \approx 78°$) are to the right of the experimental results ($\xi \approx 70°$). The real and imaginary parts of $T^{\mathrm{CB1}}_{\mathbf{k},1s}$ intersect at an angle close to the angle of the deep minimum, and at the intersection point they are close to zero but not zero. Thus, the deep minimum in the measurements of the TDCS corresponds to where $T^{\mathrm{CB1}}_{\mathbf{k},1s}$ is very small. However, by reducing ψ slightly to 66.14°, we obtain with the CB1 and modified CB1 approximations a

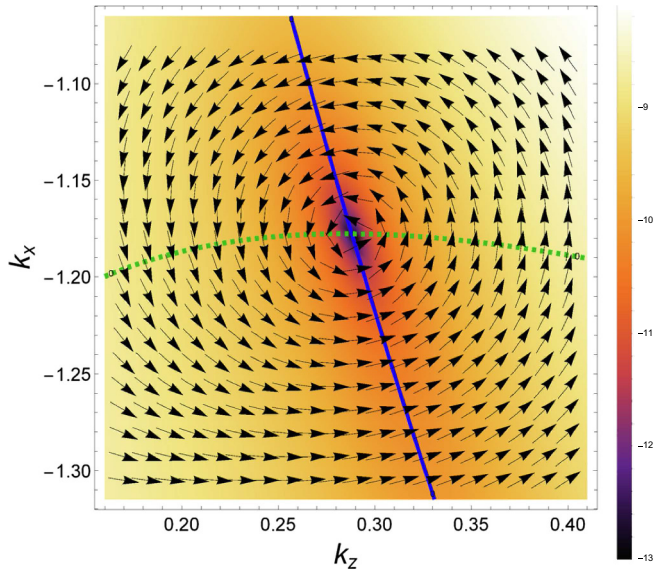

Fig. 3. A density plot of $\ln|T^{\mathrm{CB1}}_{\mathbf{k},1s}|$ for electron-impact ionization of helium for a fixed incident energy of 64.6 eV, gun angle ψ of 67.88° and a grid in the z- and x-components of the momentum of the ejected electron $\mathbf{k}$, (k_z, k_x). The nodal lines of $\mathrm{Re}[T^{\mathrm{CB1}}_{\mathbf{k},1s}]$ and $\mathrm{Im}[T^{\mathrm{CB1}}_{\mathbf{k},1s}]$ are shown respectively, by the blue solid line and green dashed line. The direction of the velocity field $\hat{\mathbf{v}}/|\mathbf{v}|$ is indicated by arrows.

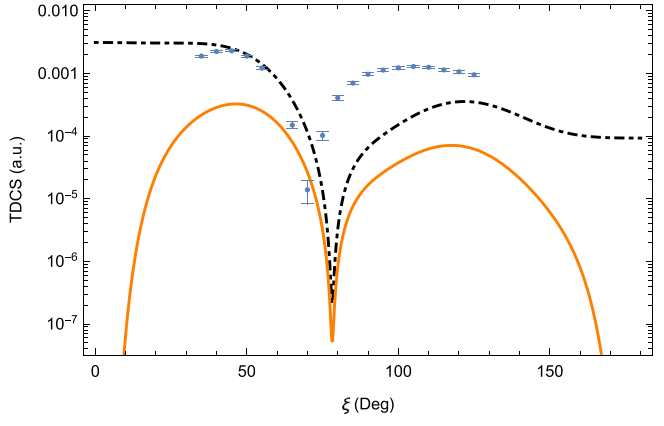

Fig. 4. The TDCS for electron-impact ionization of helium, at an incident energy of 74.6 eV and a gun angle of 67.5°, verses the polar angle ξ. The modified CB1 and the CB1 approximations are represented by the solid orange line and the black dot-dashed lines, respectively, while the experimental data which has error bars are represented by the blue dots [1–3,36,37].

very deep minimum in the TDCS corresponding to a zero in $T^{\mathrm{CB1}}_{\mathbf{k},1s}$ that occurs at $\xi \approx 78°$.

For electron-impact ionization for $E_i = 74.6$ eV and $\psi = 66.14°$, we determine $T^{\mathrm{CB1}}_{\mathbf{k},1s}$ for a uniform grid in both k_z and k_x and the velocity field corresponding to this $T^{\mathrm{CB1}}_{\mathbf{k},1s}$. We show in Figure 5 the density plot of $\ln|T^{\mathrm{CB1}}_{\mathbf{k},1s}|$, the nodal lines of $\mathrm{Re}[T^{\mathrm{CB1}}_{\mathbf{k},1s}]$ and $\mathrm{Im}[T^{\mathrm{CB1}}_{\mathbf{k},1s}]$, and the direction of the velocity field $\hat{\mathbf{v}} = \hat{\mathbf{v}}/|\mathbf{v}|$ with the arrows. There is a vortex in the velocity field and the direction of rotation around the zero is anticlockwise, which is the same

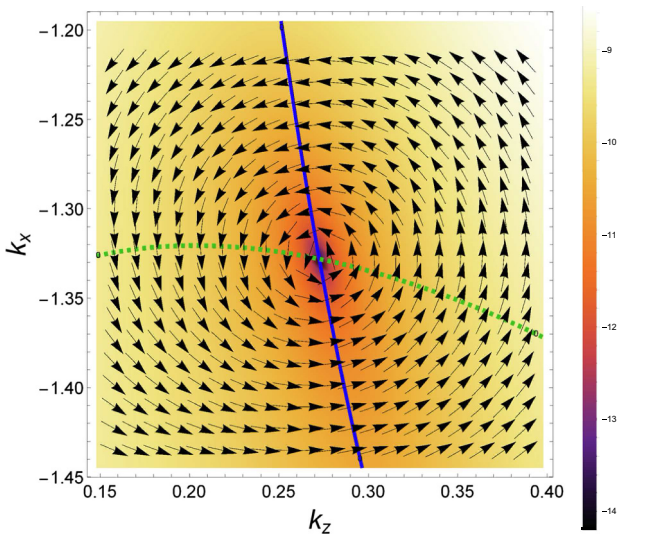

Fig. 5. The density plot of $\ln|T^{\mathrm{CB1}}_{\mathbf{k},1s}|$ for electron-impact ionization of helium for a fixed incident energy of 74.6 eV, gun angle of 66.14° and a grid in the z- and x-components of the momentum of the ejected electron $\mathbf{k}$, (k_z, k_x). The nodal lines of $\mathrm{Re}[T^{\mathrm{CB1}}_{\mathbf{k},1s}]$ and $\mathrm{Im}[T^{\mathrm{CB1}}_{\mathbf{k},1s}]$ are shown by the blue solid line and green dashed line, respectively. The direction of the velocity field $\hat{\mathbf{v}}/|\mathbf{v}|$ is indicated by arrows.

direction of rotation of the velocity field for the lower incident energy of 64.6 eV. As for the lower energy, for 74.6 eV, the circulation is 2π and $\mathrm{Im}[b] > 0$ for a linear fit (Eq. (5)) of $T^{\mathrm{CB1}}_{\mathbf{k},1s}$.

We also consider the two other incident energies of 44.6 eV and 54.6 eV that were used in the experiment [1]. While in the measurements for the energy of 54.6 eV, a deep minimum was obtained for $\psi = 67.5°$ and $\xi \approx 70°$, we obtain the deepest minimum in the CB1 and modified CB1 TDCSs that corresponds to a zero in $T^{\mathrm{CB1}}_{\mathbf{k},1s}$ and a vortex in the velocity field associated with $T^{\mathrm{CB1}}_{\mathbf{k},1s}$ for $\psi = 70.25°$ and $\xi = 73.3°$. We find a minimum in the CB1 and modified CB1 TDCSs for $E_i = 44.6$ eV and for gun angles of 60° and 75° degrees, which are the angles used in the experimental set up [1]. However, we obtain the deepest minimum in the CB1 and modified CB1 TDCSs for 44.6 eV for $\psi = 73.54°$ and $\xi = 69.3°$, and this minimum is due to a zero in $T^{\mathrm{CB1}}_{\mathbf{k},1s}$.

The CB1 gives a minimum in the TDCS for the energies of 54.6 eV, 64.6 eV and 64.6 eV and $\psi = 67.5°$ that is at a slightly larger polar angle ξ than that obtained experimentally. We find that there is a deeper minimum in the CB1 TDCS that corresponds to a zero in $T^{\mathrm{CB1}}_{\mathbf{k},1s}$ for each of these three incident energies but for different gun angles than those used in the experiment. Interestingly, at the particular energy of 64.6 eV, the minimizing gun angle of $\psi = 67.88°$ is almost the same as the gun angle of 67.5° used in the experiment. This helps explain why the minimum in the measurements of the TDCS taken at $\psi = 67.5°$ was deepest for the incident energy of 64.6 eV.

We determine for incident energies of 44.6–79.6 eV the position of a deep minimum in the CB1 and modified CB1 TDCSs. We show these positions in Figure 6 and

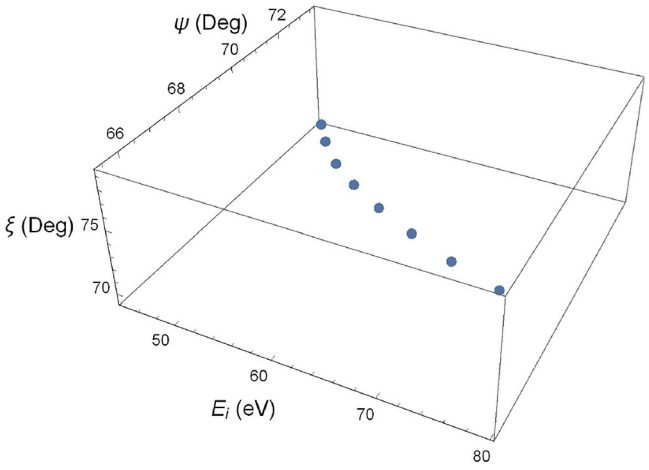

Fig. 6. The points give the position (ψ and ξ) for a deep minimum in the CB1 TDCS and modified CB1 TDCS for different incident energies E_i.

Table 1. The position (ψ and ξ) for a deep minimum in the CB1 TDCS and modified CB1 TDCS for different incident energies E_i.

E_i (eV)	Gun angle ψ (°)	Polar angle ξ (°)
44.6	73.54	69.3
49.6	71.77	71.6
54.6	70.25	73.4
59.6	68.97	75.0
64.6	67.88	76.3
69.6	66.96	77.4
74.6	66.14	78.4
79.6	65.44	79.3

in Table 1. A smooth curve would pass through the loci of points. For each of the kinematics of Table 1, we determine the velocity field and we find for each energy the direction of the velocity field around the zero in $T^{\rm CB1}_{\mathbf{k},1s}$ is anticlockwise.

For each of the kinematics of Table 1 that gives a zero in $T^{\rm CB1}_{\mathbf{k},1s}$ for electron-impact ionization of helium, there is no zero in $T^{\rm CB1}_{\mathbf{k},1s}$ for positron-impact ionization of helium.

3.2 Deep minimum in the TDCS for positron-impact ionization of helium

We consider positron-helium ionization in the coplanar plane (see Fig. 7) for the doubly symmetric geometry, where the energy is shared equally between the scattered positron and ejected electron and these outgoing particles have same polar angle. We take the z-axis to be parallel to the direction of momentum of the incident positron $\mathbf{K}_i$ and the x-axis to be in the scattering plane, defined by $\mathbf{K}_i$ and $\mathbf{K}_f$.

As we show in Figure 8, we obtain a deep minimum in the CB1 and the modified CB1 TDCSs for $E_i = 205.25$ eV and $\xi = 142.3°$. The reasonable agreement of the CB1 and

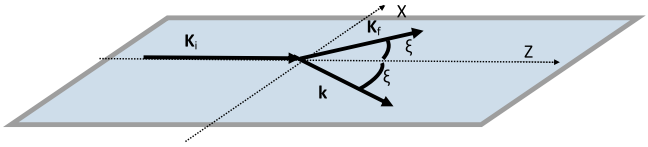

Fig. 7. Symmetric coplanar plane geometry for positron-impact ionization of helium.

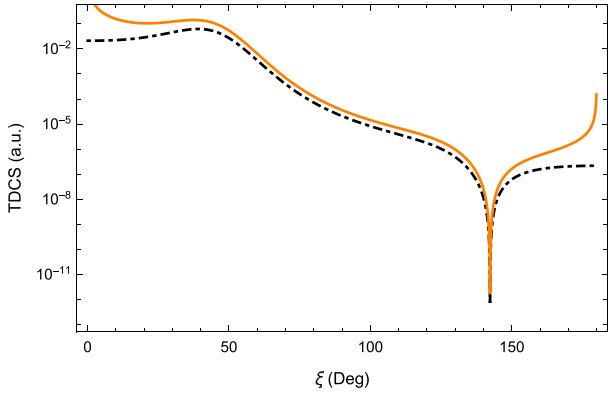

Fig. 8. The TDCS for positron-impact ionization of helium at 205.25 eV and in the coplanar doubly symmetry geometry, verses the polar angle ξ, computed using the modified CB1 (the solid orange line) and the CB1 (the black dot-dashed line) methods.

modified CB1 results with the TDCC results and experimental data for electron-helium ionization gives confidence in applying the approximate methods to compute the TDCS for positron-helium ionization at the same energy or higher. For the deep minimum in positron-impact ionization, in contrast to that for electron-impact ionization, the z-components of the momenta of the outgoing particles are negative. The deep minimum in the TDCS is due to a zero in $T^{\rm CB1}_{\mathbf{k},1s}$ at $\xi = 142.3°$.

We determine the $T^{\rm CB1}_{\mathbf{k},1s}$ and velocity field $\mathbf{v}$ for a uniform grid in (k_z, k_x), for the case where we take the polar angles of the two outgoing particles to be the same (Fig. 7) and we fix E_i at 205.25 eV. To satisfy energy conservation, as the energy of the ejected electron is varied, we adjust the energy of the scattered positron E_f accordingly. In Figure 9, we show a density plot of $\ln|T^{\rm CB1}_{\mathbf{k},1s}|$, the nodal lines of $T^{\rm CB1}_{\mathbf{k},1s}$, and the direction of the velocity field $\hat{\mathbf{v}} = \hat{\mathbf{v}}/|\mathbf{v}|$ by the arrows. The nodal lines intersect at the zero in $T^{\rm CB1}_{\mathbf{k},1s}$ which is where the TDCS has its deep minimum. The velocity field lines rotate clockwise around the zero in $T^{\rm CB1}_{\mathbf{k},1s}$ (the intersection point of the nodal lines) where the TDCS is the deepest. Interestingly, the direction of rotation is in the opposite direction to that for electron-helium ionization. This maybe due to different kinematics and to the positon of the zero in $T^{\rm CB1}_{\mathbf{k},1s}$. Since the rotation is clockwise for positron-impact ionization, the value of the circulation is -2π. This is consistent with $\mathrm{Im}[b] < 0$ which we obtain by fitting $T^{\rm CB1}_{\mathbf{k},1s}$ to the linear form of equation (5). According to equation (7), for $\mathrm{Im}[b] < 0$, the expectation value of the $\hat{y}$-component of the

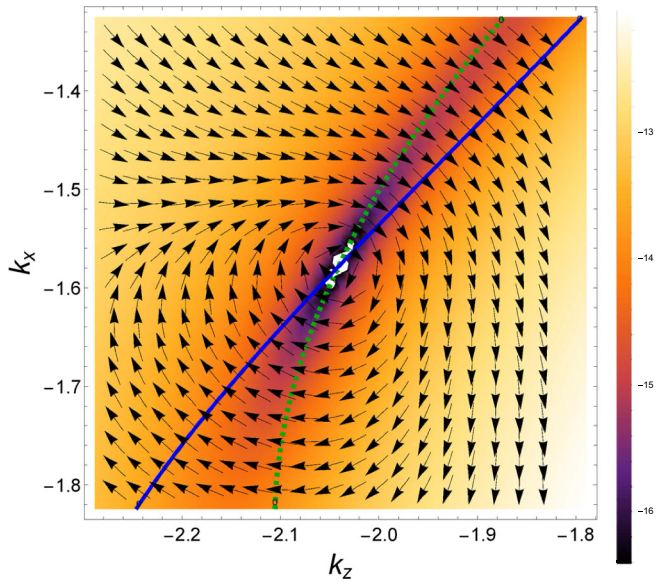

Fig. 9. The density plot of $\ln|T^{\mathrm{CB1}}_{\mathbf{k},1s}|$ for positron-impact ionization of helium for a fixed incident energy of 205.25 eV in the coplanar doubly symmetry geometry and a grid in the z- and x-components of the momentum of the ejected electron $\mathbf{k}$, (k_z, k_x). The nodal lines of $\mathrm{Re}[T^{\mathrm{CB1}}_{\mathbf{k},1s}]$ and $\mathrm{Im}[T^{\mathrm{CB1}}_{\mathbf{k},1s}]$ are shown by the blue solid line and green dashed line, respectively. The direction of the velocity field $\hat{\mathbf{v}}/|\mathbf{v}|$ is indicated by arrows.

angular momentum operator for a small area that includes the zero in $T^{\mathrm{CB1}}_{\mathbf{k},1s}$ is negative.

For electron-impact ionization of helium, we determine $T^{\mathrm{CB1}}_{\mathbf{k},1s}$ for the kinematics and geometry of where we obtain a zero in $T^{\mathrm{CB1}}_{\mathbf{k},1s}$ for positron-impact ionization of helium. However, we find that there is no zero in $T^{\mathrm{CB1}}_{\mathbf{k},1s}$ for this energy and geometry.

4 Summary

The deep minima in the experimentally measured TDCS for electron-impact ionization of helium at the incident energies of 54.6 eV, 64.6 eV and 74.6 eV in the doubly symmetric out-of-the plane geometry are due to kinematics that are close to the kinematics that give zeros in $T^{\mathrm{CB1}}_{\mathbf{k},1s}$. By adjusting ψ for each energy, we obtain very deep minima in the CB1 and modified CB1 TDCSs and corresponding zeros in $T^{\mathrm{CB1}}_{\mathbf{k},1s}$. The zeros in $T^{\mathrm{CB1}}_{\mathbf{k},1s}$ correspond to vortices in the velocity field associated with $T^{\mathrm{CB1}}_{\mathbf{k},1s}$. The expectation value of the angular momentum in the vicinity of a zero in $T^{\mathrm{CB1}}_{\mathbf{k},1s}$ is nonvanishing. We found that the minimizing gun angle is closest to the gun angle of 67.5° for the energy of 64.6 eV, which helps explain why the minimum is deepest in the measured TDCS for this incident energy.

We determined for incident energies E_i of 44.6–79.6 eV, in steps of 5 eV, ψ and ξ for a deep minimum in the CB1 and modified CB1 TDCSs that corresponds to a zero in $T^{\mathrm{CB1}}_{\mathbf{k},1s}$. We computed the velocity field $\mathbf{v}$ for these energies and we found that for each energy this field rotates anticlockwise around each zero.

The CB1 and modified CB1 results of the TDCS for electron-impact ionization of helium at 64.6 eV and $\psi = 67.5°$ are in reasonable accord with the TDCC [7] and experimental measurements [1], and at 74.6 eV and $\psi = 67.5°$ with experimental measurements, although the polar angles for the minima in the CB1 and modified CB1 results are larger than in the TDCC and experimental results.

Interestingly, using the CB1 and modified CB1 approximations, we obtain a deep minimum in the TDCS for positron-impact ionization of helium at 205.25 eV in the coplanar doubly symmetric geometry. The deep minimum in the TDCS at $\xi = 142.3°$ is due to a zero in $T^{\mathrm{CB1}}_{\mathbf{k},1s}$. Corresponding to this zero, there is a vortex in the velocity field that rotates clockwise around the zero.

The velocity field for the two projectiles for the same target helium rotates in opposite directions and thus the value of the circulation differs by a sign.

We appreciate discussions with Drs. James Colgan, Gaetana (Nella) Laricchia and Don Madison. We are thankful for the theoretical 3DW and TDCC results from the paper [7] provided by Dr. James Colgan and experimental data from the paper [1] provided by Dr. Andrew Murray. We also appreciate Coulomb-Born codes from Dr. Javier Botero. S. J. W. is thankful for support from the NSF under grant No. PHYS-1707792. Mathematica [38] and Microsoft Publisher [39] were used for the figures.

5 Author contribution statement

All authors conducted research for the project presented in the manuscript. C. M. DeMars and S. J. Ward prepared the manuscript, and S.J. Ward supervised the project.

References

1. A.J. Murray, F.H. Read, Phys. Rev. A **47**, 3724 (1993)
2. A.J. Murray, F.H. Read, J. Phys. B: At., Mol. Opt. Phys. **26**, L359 (1993)
3. A.J. Murray, F.H. Read, Phys. Rev. Lett. **69**, 2912 (1992)
4. J. Berakdar, J.S. Briggs, J. Phys. B: At., Mol. Opt. Phys. **27**, 4271 (1994)
5. J. Berakdar, J.S. Briggs, Phys. Rev. Lett. **72**, 3799 (1994)
6. J. Rasch, C.T. Whelan, R.J. Allen, S.P. Lucey, H.R.J. Walters, Phys. Rev. A **56**, 1379 (1997)
7. J. Colgan, O. Al-Hagan, D.H. Madison, A.J. Murray, M.S. Pindzola, J. Phys. B: At., Mol. Opt. Phys. **42**, 171001 (2009)
8. J.H. Macek, J.B. Sternberg, S.Y. Ovchinnikov, J.S. Briggs, Phys. Rev. Lett. **104**, 033201 (2010)
9. I. Bialynicki-Birula, Z. Bialynicka-Birula, C.Śliwa, Phys. Rev. A **61**, 032110 (2000)
10. J. H. Macek, in *Dynamical processes in atomic and molecular Physics* (Bentham Science, Sharjah, UAE, 2012), Chap. 1, pp. 3–28

11. K.-K. Kan, J.J. Griffin, Phys. Rev. C **15**, 1126 (1977)
12. S.K. Ghosh, B.M. Deb, Phys. Rep. **92**, 1 (1982)
13. J.M. Feagin, J. Phys. B: At., Mol. Opt. Phys. **44**, 011001 (2011)
14. S.J. Ward, J.H. Macek, Phys. Rev. A **90**, 062709 (2014)
15. J. Botero, J.H. Macek, Phys. Rev. A **45**, 154 (1992)
16. J. Botero, J.H. Macek, J. Phys. B: At., Mol. Opt. Phys. **24**, L405 (1991)
17. J.H. Macek, J. Botero, Phys. Rev. A **45**, R8 (1992)
18. J. Botero, J.H. Macek, Phys. Rev. Lett. **68**, 576 (1992)
19. F. Navarrete, R. Della Picca, J. Fiol, R.O. Barrachina, J. Phys. B: At., Mol. Opt. Phys. **46**, 115203 (2013)
20. F. Navarrete, R.O. Barrachina, J. Phys. B: At., Mol. Opt. Phys. **48**, 055201 (2015)
21. F. Navarrete, R.O. Barrachina, Nucl. Instrum. Phys. Res. B **369**, 72 (2016)
22. F. Navarrete, R.O. Barrachina, J. Phys.: Conf. Ser. **875**, 012022 (2017)
23. A.W. Alrowaily, S.J. Ward, P. Van Reeth, J. Phys. B: At., Mol. Opt. Phys. **52**, 205201 (2019)
24. J.H. Macek, AIP Conf. Proc. **1525**, 111 (2013)
25. S.Y. Ovchinnikov, J.H. Macek, D.R. Schultz, Phys. Rev. A **90**, 062713 (2014)
26. C.M. DeMars, J.B. Kent, S.J. Ward, Bull. in Am. Phys. Soc. **64**, N°4, 119 (2019) http://meetings.aps.org/Meeting/DAMOP19/Session/L01.13
27. S. J. Ward, http://meetings.aps.org/Meeting/GEC19/Session/LW1.6
28. C.M. DeMars, S.J. Ward, Deep Minima in the TDCS for Positron-helium ionization computed using the Coulomb-Born approximation, in *XX International Workshop on Low-Energy Positron and Positronium Physics, POSMOL 2019 Book of Abstracts, Serbia, 18–21 July 2019*, edited by D. Cassidy, M.J. Brunger, Z.L. Petrović, S. Dujko, B.P. Marinković, D. Marić, S. Tošić (Serbian Academy of Sciences and Arts, 2019) LEPPP 12, p. 53
29. Á. Kövér, D.J. Murtagh, A.I. Williams, G. Laricchia, J. Phys.: Conf. Ser. **199**, 012020 (2010)
30. X. Zhang, C.T. Whelan, H.R.J. Walters, J. Phys. B: At., Mol. Opt. Phys. **23**, L173 (1990)
31. X. Zhang, C.T. Whelan, H.R.J.Walters, J. Phys. B: At., Mol. Opt. Phys. **23**, L509 (1990)
32. S.J. Ward, J.H. Macek, Phys. Rev. A **49**, 1049 (1994)
33. J. Berakdar, H. Klar, J. Phys. B: At., Mol. Opt. Phys. **26**, 3891 (1993)
34. D.R. Bates, G. Griffing, Proc. R. Soc. A **66**, 961 (1953)
35. https://physics.nist.gov/PhysRefData/Handbook/Tables/heliumtable1.htm (Date accessed September 24, 2019).
36. http://es1.ph.man.ac.uk/Atomic_%26_Molecular_Physics/Home_page.html (Date accessed October 14, 2019)
37. Professor Andrew Murray, *Private Communication* (2019)
38. Wolfram Research, Inc., Mathematica (Wolfram Research, Inc., Champaign, IL)
39. Publisher, Microsoft Office 365 ProPlus